Hydrological impacts of mesquite encroachment in the upper San Pedro watershed

W. Nie, Y. Yuan*, W. Kepner, C. Erickson, M. Jackson

USEPA NERL, Landscape Ecology Branch, Environmental Sciences Division, 944 East Harmon Avenue, Las Vegas, NV 89119, USA

ABSTRACT

Over the past century, mesquite trees (*Prosopis* spp.) have exhibited substantial increase in abundance throughout areas in the American Southwest that were once dominated by desert grassland. To assess hydrological consequences of mesquite encroachment, the Soil and Water Assessment Tool (SWAT) was applied to simulate progressive mesquite encroachments in the upper San Pedro watershed (U.S./Mexico). The simulated average annual basin evapotranspiration (ET) increases with mesquite encroachment, leading to the decrease of annual water yield and percolation by 9.8% and 9.7%, respectively. Substantial increase of ET (up to 19.19 mm) and decrease of percolation, and surface runoff (to -12.90 and -3.20 mm, respectively) were observed in the southeast, middle-west, and northern subwatersheds of the basin and the most significant decrease of surface runoff (around -35.8%) was simulated during the wet period. In addition, a non-linear hydrological response relative to mesquite encroachment was observed, i.e. hydrological processes changed markedly until a certain amount (approximately 40%) of grassland was removed, indicating that the strongest increase of ET occurred in the earliest stages of encroachment. Consequently, changes in vegetation physiognomy, such as mesquite encroachment, have broad implications for landuse management especially in regard to reliable water supplies in arid and semi-arid environments.

Published by Elsevier Ltd.

1. Introduction

Extensive encroachments of mesquite into grassland and savannas occurred throughout the arid and semi-arid regions of the world over the last several decades or earlier (Briggs et al., 2007; Goslee et al., 2003; Shiferaw et al., 2004; van Klinken et al., 2006). Two species of mesquite tree, i.e. velvet mesquite (*Prosopis velutina*) and honey mesquite (*Prosopis glandulosa*), have demonstrated significant expansion into the desert grasslands of the Southwestern United States (Wilson et al., 2001). Most of the information regarding phase-transition of desert grassland to indigenous mesquite woodland has been derived from anecdotal accounts of rangeland users and managers or via the technique of repeat photography (Bahre, 1991; Grover and Musick, 1990; Hastings and Turner, 1965; West and Vásquez-León, 2008). Regional change has also been documented via satellite remote sensing (Kepner et al., 2000, 2002). The conversion of grassland into mesquite can generate many environmental consequences through altering water and nutrient cycling, changing carbon

storage, enhancing climate variability, and reducing biodiversity (Ceballos et al., 2010; Jackson et al., 2002; Schlesinger et al., 1990; Zeng et al., 1999). More specifically, considering that water is the limiting resource for the ecosystem in semi-arid and arid regions, hydrological response to mesquite encroachment may directly impact the availability of ecosystem services and consequently human well being. Impacts of Land Use and Land Cover (LULC) change on hydrology in regions with mesquite encroachment have been investigated (Hernandez et al., 2003; Miller et al., 2007; Nie et al., 2011; Saleh et al., 2009; Stromberg et al., 1993). However, simultaneous changes in LULC, such as grassland conversion to mesquite woodland and to urbanized areas increases the difficulty of quantifying the effects of mesquite encroachment alone on hydrological cycling. To address this issue, a series of land cover change scenarios were developed to represent progressive conversion of grassland to mesquite woodland and the Soil and Water Assessment Tool (SWAT) model (Arnold and Fohrer, 2005; Arnold et al., 1998; Gassman et al., 2007; Neitsch et al., 2005a; Srinivasan et al., 1998) was employed to simulate hydrological consequences of the developed LULC scenarios. The objective of this study is to quantify how mesquite encroachment influences the major hydrological processes at the basin scale. Although this study does not provide explicit recommendations for resource

* Corresponding author. Tel.: +1 702 798 2112.
  E-mail address: yuan.yongping@epa.gov (Y. Yuan).

managers, the intent is to contribute scientific understanding that can be used toward environmental decision-making. This is especially relative to the potential impact of landscape change on water provisioning, a vital ecosystem service in the American Southwest.

2. Study site

Extensive mesquite encroachment occurred in the upper San Pedro River basin from 1973 to 1986: proportional extent of mesquite increased from 2.81% to 14.33% and grassland decreased from 41.07% to 35.00% (Kepner et al., 2000). The extensive vegetation change and satellite documentation in this watershed makes it an ideal study site for the present research.

The upper San Pedro watershed originates in Sonora, Mexico near Cananea and flows north into southeastern Arizona, USA (Fig. 1). The drainage area for the upper San Pedro watershed is approximately 7400 km^2. Elevations in the watershed range from 900 to 2900 meters, and annual rainfall ranges from 300 to 750 mm (Ghan et al., 2006). The LULC in the river basin includes woodland (oak and mesquite), desertscrub, grassland, forest, agriculture crops, riparian, and urban (Kepner et al., 2000).

3. Method and data

In this study, the SWAT model was calibrated and validated and then was used to simulate a series of designed LULC scenarios, which represent progressive encroachment of mesquite woodland into desert grassland. Hydrological consequences of mesquite encroachment were evaluated by running the calibrated SWAT models with a constant Digital Elevation Model (DEM), soil data, and meteorological forcing, while changing only the digital LULC data.

3.1. Model description

The SWAT model is a continuous, long-term, physically based semi-distributed model developed to assess impacts of climate and land management on hydrological processes, sediment loading, and pollution transport in watersheds (Arnold et al., 1998). In the SWAT model, a watershed is divided into subwatersheds or subbasins, which are further partitioned into a series of hydrological response units (HRUs). HRUs are uniform units that share unique combinations of soil and land use. Hydrological components, sediment yield, and nutrient cycles are simulated for each HRU and then aggregated for the subbasins.

The hydrological cycle simulated in SWAT is based on the water balance equation:

$$SW_t = SW_0 + \sum_{i-1}^{t} \left(R_{day} - Q_{surf} - E_a - w_{seep} - Q_{gw} \right) \tag{1}$$

where, SW_t and SW_0 are the final and initial soil water content on day i (mm H$_2$O), t the time steps on day i, R_{day} the rainfall that reaches the soil surface on day i (mm), Q_{surf} the surface runoff on day i (mm), E_a the evapotranspiration on day i (mm), w_{seep} the
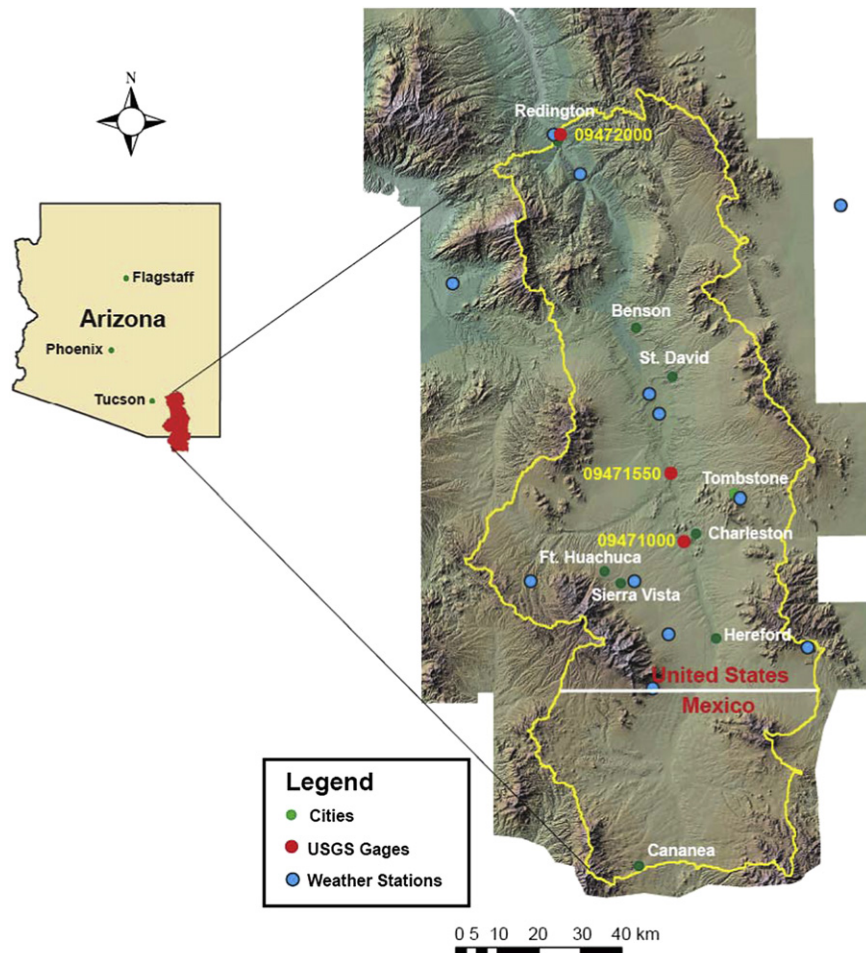

Fig. 1. Locations of rural and municipal areas, USGS monitoring gages, and weather stations in the upper San Pedro watershed (modified from Kepner et al., 2000).

interflow on day i (mm), and Q_{gw} is the baseflow on day i (mm) (Neitsch et al., 2005).

The simulated hydrological components include evapotranspiration (ET), surface runoff, percolation, lateral flow, groundwater flow (return flow), transmission losses, ponds, and water yield (Arnold et al., 1998). Evaporation and transpiration are simulated separately in SWAT: evaporation is computed using exponential functions of soil depth and water content and transpiration is estimated using a linear function of potential evapotranspiration (PET) and leaf area index. Three methods can be used to estimate PET: Hargreaves (Hargreaves et al., 1985), Priestley–Taylor (Priestley and Taylor, 1972), and Penman–Monteith (Monteith, 1965). The Pennman–Monteith method was used to calculate PET in this study. Surface runoff is simulated using a modification of the Soil Conservation Service (now the Natural Resources Conservation Service) Curve Number (SCS-CN) method (USDA, 1972) with daily rainfall. Curve number values used for runoff estimation are based on soil type, LULC, and land management conditions (Rallison and Miller, 1981) and are adjusted according to soil moisture conditions (Arnold et al., 1993). Percolation is estimated using the combination of a storage routing technique and a crack-flow model (Arnold et al., 1998). The lateral flow is estimated simultaneously with percolation using a kinematic storage model (Solan et al., 1983). The groundwater flow (baseflow) into a channel is calculated based on hydraulic conductivity of shallow aquifer, distance from subbasin to main channel, and water table height (Hooghoudt, 1940). Transmission loss, amount of water removed from tributary channels by transmission, is calculated using procedure described in SCS Hydrology Handbook (Lane, 1983). Water yield, total amount of water leaving the HRU and entering main channel, is equal to surface runoff plus lateral flow and baseflow, and minus transmission loss and pond abstractions (Neitsch et al., 2005b).

3.2. Land use and land cover scenario design

Mesquite encroachment occurred throughout the arid and semi-arid regions of the world over the last several decades (Briggs et al., 2007; Goslee et al., 2003; Shiferaw et al., 2004; van Klinken et al., 2006). To investigate hydrological impacts of mesquite encroachment, a series of LULC change scenarios were developed with progressive conversion of mesquite from grassland. These developed scenarios represent the trend of steady increase of the numbers of polygons (patches), patch size, and the connectivity of mesquite woodland in the upper San Pedro River basin identified by remote images (Kepner et al., 2002). Using the 1973 digital LULC map developed via North American Landscape Characterization (NALC) project data (Kepner et al., 2002) as a basis, gradual LULC changes were designed to simulate the patterns of the past in the San Pedro (Kepner et al., 2002, 2000) which provide predictive inference (i.e. a change model) for evaluating projected trends. We considered 11 degrees of change, including approximate 0, 10, 20, 30, 40, 50, 60, 70, 80, 90, and 100%, where 100% was regarded as complete replacement of grassland with mesquite. In each step, the area of grassland was reduced by approximate 10% to balance the expansion of mesquite, while the remainder of the LULC remained unchanged.

The scenarios were developed by following procedure in ArcGIS: 1) extract mesquite and grassland from 1973 digital LULC map, and reclassify grassland into mesquite (raster1, 100% mesquite); 2) use "shrink" tool in GIS to obtain correct percentage of mesquite (10%–50%); 3) mosaic the derived raster using a raster with only grassland (reclassified from raster1 to a raster with 0% mesquite); 4) since the shrink tool only works up to 50%, we used tool "expand" to obtain correct percentages of mesquite for the rest of scenarios (60%–90%).

3.3. Model input preparation

The basic SWAT model inputs include a DEM, soil data, LULC data, and meteorological data. The DEM was derived from the National Elevation Dataset (NED) of USGS with 1 arc-second resolution (Gesch et al., 2002), and the soil data was from the State Soil Geographic (STATSGO) database. The LULC data of 1973, 1992 and 1997 used for this study was from the NALC project (Landsat Multi-Spectral Scanner) and Landsat Thematic Mapper (Kepner et al., 2002; USEPA, 1993). For climate information, daily maximum and minimum temperature, precipitation, solar radiation, relative humidity and wind speed are needed to account for temporal variation in weather. This data can be historically measured, generated using the SWAT built in WXGEN weather generator model (Sharpley and William, 1990), or supplied to SWAT using a combination of the two methods. For this study, daily precipitation and minimum-maximum temperature from Jan. 1960 to Apr. 2008 were acquired from the National Climatic Data Center (NCDC). Twelve meteorological stations were found within or nearby the upper San Pedro watershed (Fig. 1). Missing records of daily observations of precipitation and minimum-maximum temperature were interpolated from weather data within a radius of 25 miles using the method developed by Di Luzio et al. (2008). The remainder of the weather information (solar radiation, relative humidity and wind speed) used in SWAT simulation was generated by the WXGEN weather generator model (Sharpley and William, 1990).

The area for stream definition was set as 3500 ha, upon which the upper San Pedro River basin was divided into 116 subbasins. The divided subbasins matched 12-digit HUCs in the upper San Pedro watershed. The subbasins were further divided into HRUs based on the land use, soil, and slope types (0.1%, 1%, and 5%). The number of HRUs differs when different LULC maps are employed. As an example, the numbers of HRUs for 1992 and 1997 LULC are 2146 and 2225, respectively. There are 10 classes of LULC and 23 soil types in the upper San Pedro watershed. Watershed parameterization includes the calculation of subbasin geometry parameters from DEM and the assigning values to the HRUs through the inner database. The database for the SWAT model includes parameter values for crops, urban, and soils, such as CN2 values (SCS runoff curve number for moisture condition II), SOL_AWC (Available water capacity of the soil layer), LAI (leaf area index), and other soil physical and hydraulic properties. Values were assigned to each HRU based on its LULC class and soil type during the parameterization process. The simulation was initialized by setting default values of each parameter; a five year warm up period was applied to erase the impact of initial condition for the model calibration and validation.

3.4. Model calibration and validation

Simulations for model calibration were set up using 1992 NALC LULC data. Annual (water year) and monthly streamflow from Oct. 1986 to Sept. 1995 at two USGS gages (Redington and Charleston, Fig. 1) were used for model calibration. After model calibration, simulations for model validation were set up using 1997 Landsat Thematic Mapper LULC data; and annual (water year) and monthly streamflow at Tombstone (Oct. 1996–Sept. 2005) and Charleston (Oct. 1995–Sept. 2005) were used for model validation. The model was calibrated manually and three criteria were used to evaluate performance of model calibration/validation.

3.4.1. Manual calibration processes

The model was calibrated by manually editing sensitive parameters for hydrological components (surface runoff, baseflow, lateral flow, ET, and channel transmission loss). In this study, the lateral flow was assumed to be zero, because no obvious impervious layers

in soil profiles, such as black shales, which were pre-required for the lateral flow to be generated, were observed in the watershed. In the SWAT model, the lateral flow was reduced to a very low level (close to zero) by changing the adjust factor for lateral flow (Adjf_latq) from the default value of 1 into 0.02. Baseflow should be a very small portion recharging back to the stream because very large portions of the upper San Pedro River are ephemeral. At the Redington gage (down-stream), the river only contains water during and immediately after a storm event and is dry the rest of the year. At Tombstone and Charleston gage (upper-stream), although the river flows intermittently, the water supply may not be from baseflow for the relatively higher elevation (corresponding to deeper groundwater table level values) than downstream. Thus, we eliminated the baseflow in the SWAT model by reducing threshold water level in the shallow aquifer for re-evaporation (Revapmn) and enhancing the re-evaporation coefficient and threshold water level in shallow aquifer for baseflow (GWQMN). Surface runoff is the major water supply for the watershed. Whereas, we noticed that streamflows were often under-estimated for light rainfall events and over-estimated for large rainfall events. Woodward et al. (2004) found that runoff estimates could be enhanced for relatively light rainfalls and be reduced for relative large rainfalls by changing the initial abstraction ratio to be 0.05 from its originally defined value of 0.2. Thus, to calibrate surface runoff, we set the initial abstraction ratio to be 0.05 and edited the CN2 (SCS runoff curve number) to a relatively low value to match the change of initial abstraction ratio. Channel transmission loss is a large portion (4%–100%) of the water balance in the Walnut Gulch Experimental Watershed, a sub-watershed of the upper San Pedro River basin (Cataldo et al., 2005). USGS records show that monthly streamflow (in volume) at downstream locations (Redington gage) is not always larger than in upperstream (Tombstone and Charleston gages), indicating that transmission loss exists for the major channel (stream order 4 and 5). However, it's hard to quantify the ratio of channel transmission loss to the basin recharge. In this study, we assume approximately half of the water yield was lost through transmission loss during channel routing processes. To calibrate the transmission loss, we set the TRNSRCH (Fraction of transmission loss partitioned into deep aquifer) to be 1 and manually edited effective hydraulic conductivity of channel (CH_K2). The optimal values for SWAT calibration are listed in Table 1.

3.4.2. Performance evaluation criteria

Three criteria were used to evaluate the model's performance on calibration and validation: Nash-Sutcliff (NS) coefficient (Nash and Sutcliffe, 1970), coefficient of determination (R^2), and percent bias (PBIAS) (Gupta et al., 1999). The calibration and validation performance for the SWAT model is considered satisfactory when R^2 and NS are greater than 0.5 (Moriasi et al., 2007). When the absolute value of PBIAS is less than 15, the SWAT model is rated a good performer (Moriasi et al., 2007).

3.4.3. Model application

After model calibration and validation, simulations were run for all developed LULC scenarios with an unchanged DEM, soil data, and meteorological forcing from Jan. 1960 to Apr. 2008 (48.3 years) to evaluate hydrological consequences of mesquite encroachment in the upper San Pedro watershed.

4. Results and discussion

4.1. Calibration/validation results

The comparison between simulated and observed annual (in water year) and monthly streamflow in the periods of calibration

Table 1
Description, default and calibrated values that were used in the model calibration/validation (*, the multiple sign, means the default values of parameter are multiplied by the number following the "*").

Parameter	Default	Description	Calibrated value
Adjf_latq	1	Adjust factor for lateral flow	0.02
λ	0.2	Initial Abstraction Ratio	0.05
CN2	30–92	SCS runoff curve number for moisture condition II	*0.58
ESCO	0.95	Soil evaporation compensation factor	0.05
SOL_AWC	0.01–0.19	Available water capacity of the soil layer	*1.4
GW_Revap	0.02	Revaporation coefficient	0.2
Revapmn	1	Threshold water level in shallow aquifer for revap	0
GWQMN	0	Threshold water level in shallow aquifer for baseflow	100
TRNSRCH	0	Fraction of transmission loss partitioned into deep aquifer	1
CH_K2	0	Effective hydraulic conductivity of channel	0.6

(Oct. 1986–Sept. 1995) and validation (Oct. 1996–Sept. 2005) are shown in Figs. 2 and 3, respectively. In general, a good match can be seen between simulated and observed values. The NS and R^2 values for the annual (in water year) and monthly calibration and validation are listed in Table 2. All NS and R^2 values are above 0.5 (except NS coefficient for annual calibration at the Redington gage), and PBIAS are in the range of ±25% (except annual calibration at the Charleston gage), suggesting satisfactory model performance (Moriasi et al., 2007). Although the overall performance of the model is satisfactory as shown in Figs. 2 and 3, and Table 2, a large difference was observed for the water year of 1992 at Redington
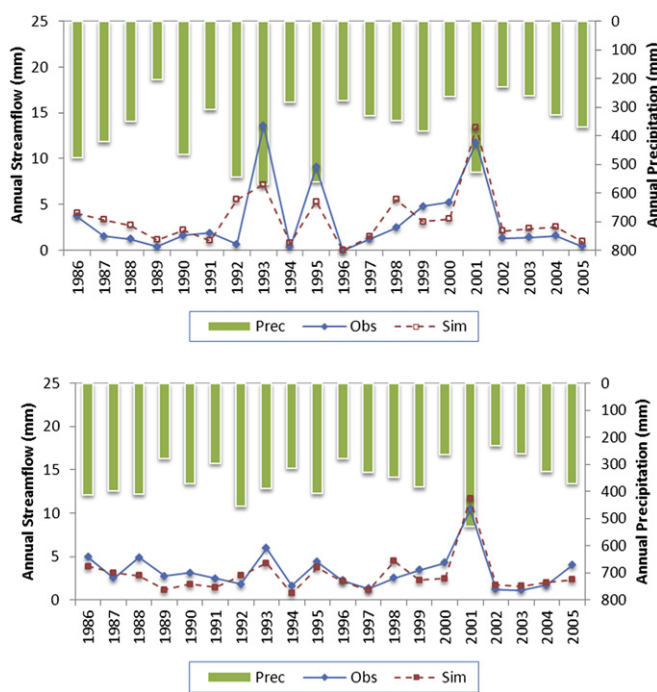

Fig. 2. Annual (in water year) precipitation and simulated and observed streamflow in the upper San Pedro Watershed. Upper: Redington (1986–1995) and Tombstone (1997–2005) gages; Lower: Charleston gage (1986–2005).
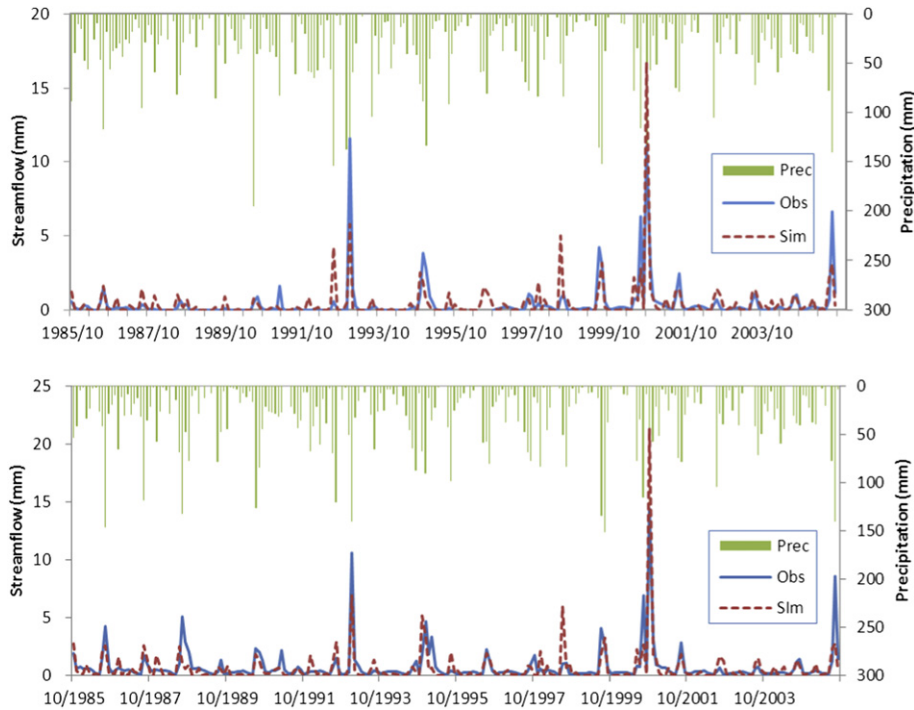
Fig. 3. Monthly precipitation and simulated and observed streamflow in the upper San Pedro watershed. Upper: Redington (10/1985–09/1995) and Tombstone (10/1996–09/2005) gages; Lower: Charleston gage (10/1985–09/2005).

and 1993 at both Redington and Charleston. Intuitively, the simulated values seem more reasonable because it matches the rainfall patterns as shown in Fig. 2. Possible reasons for the discrepancies are the limitation of the curve number method. First, high uncertainties could be generated by using daily total rainfall depth as SWAT input. As an example, a large amount of streamflow (4.21 mm) at the Redington gage on Aug. 1992 simulated in the SWAT model was mainly attributed to a daily rainfall of 127.8 mm on Aug. 24, 1992 in the downstream. Whereas, the rainfall depth on that day could be the combination of several relatively small rainfall events, which may not be able to generate significant runoff (recorded streamflow in Aug. 1992 is 0.58 mm). Second, it fails to consider the effects of duration and intensity of precipitation. For instance, runoff could be generated by some high-intensity, short-duration, limited areal extent summer thunderstorms (Simanton et al. 1996) near observation gages. Whereas, those limited areal extent summer thunderstorms may not be simulated by the SWAT model for a large extent.

Overall, the good match between simulation and observation, as well as high NS, R^2, and low absolute values for PBIAS indicates that streamflow can be described by the calibrated model. Thus, the SWAT models set up by the optimal parameters were applied to evaluate hydrological consequences to mesquite encroachments.

To further gain credence of the model, water balance was calculated for the calibration and validation periods using Eq. (1). During the model calibration period (1986–1995), the water balance

errors were −0.29 mm to 0.73 mm, with relative errors (error/precipitation) from −0.06 percent to 0.17 percent. During the model validation period (1996–2005), the absolute water balance errors were −0.54 mm to 0.08 mm, with relative errors from −0.14 percent to 0.02 percent. The small errors suggest that the calibrated model satisfies the requirement of water balance at the watershed scale.

4.2. Impacts of mesquite encroachment on hydrology

Spatial and temporal impacts of mesquite encroachment on hydrology were investigated through comparing variations of simulated hydrological processes between two extreme LULC scenarios (with or without coverage of mesquite). Scenario 0 represents a LULC map with 0% of grassland that was encroached by mesquite and Scenario 10 represents a LULC map with 100% of grassland that was encroached by mesquite (Fig. 4). Fig. 5 shows the spatial distribution of DEM, and deviations of four hydrological processes between Scenario 0 and Scenario 10. Deviations were calculated as the difference between these two scenarios for each subbasin. As an example, deviation of ET for subbasin 1 is the ET at subbasin 1 for Scenario 10 (all grassland was replaced by mesquite) minus that for scenario 0. As shown in Fig. 5, most significant variations of hydrological processes occurred in the southeast, middle-west, and northern subwatersheds of the upper San Pedro River basin. An apparent increase of ET can be observed in these subwatersheds, with an increase of annual averaged values up to

Table 2
Criteria for examining the accuracy of calibration and validation (the validation period at Tombstone gage is from Oct. 1996 to Sept. 2005).

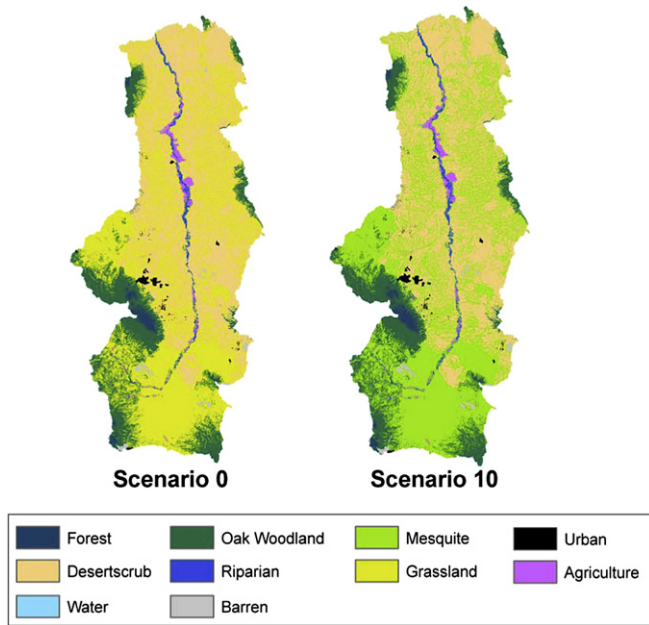| Index	Calibration (10/1985–09/1995)				Validation (10/1995–09/2005)			
	Redington		Charleston		Tombstone		Charleston	
	Yearly	Monthly	Yearly	Monthly	Yearly	Monthly	Yearly	Monthly
NS coefficient	0.45	0.56	0.82	0.52	0.94	0.57	0.93	0.55
R^2	0.66	0.57	0.66	0.55	0.84	0.70	0.82	0.70
PBIAS	1.94	−1.29	25.46	24.63	−16.27	−9.23	1.38	3.00

Fig. 4. Two Land Use and Land Cover scenarios in the Upper San Pedro Watershed. Scenario 0: 0% of grassland was replaced by mesquite; Scenario 10: 100% of grassland was replaced by mesquite.

19.19 mm. In addition, substantial decreases of annual averaged values of percolation and surface runoff were observed in these subwatersheds, with a maximum decrease of −12.90 and −3.20 mm, respectively. Impacts of mesquite encroachments on hydrology vary through time. Fig. 6 shows the relative decrease of simulated basin annual surface runoff between Scenario 0 and Scenario 10 from 1960 to 2007. Three multi-decadal precipitation

regimes are identified in the upper San Pedro River Basin: 1960–1976, 1977–1994, and 1995–2007 (Fig. 6). A wet episode is sandwiched between two dry conditions. The dry episodes in the upper San Pedro watershed are contemporaneous with observed droughts of Arizona identified using an average of monthly records from 25 U.S. historical climate network stations in Arizona from 1930–2002 (ADRW, 2010; Griffiths et al., 2006; USGS, 2004). As shown in Fig. 6, the overall decreases of streamflow between Scenario 0 and Scenario 10 in wet periods are higher than the relative decreases during streamflow in dry periods which indicates that the change of ET is higher in wet period. Therefore, precipitation is the secondary controlling factor of ET besides LULC change. As we discussed in the model calibration section, streamflow was mainly composed of surface runoff. The runoff was simulated using SCS Curve Number method in the SWAT model. Compared to grassland, mesquite is associated with a relatively smaller curve number. Theoretically, the differences between simulated runoffs for grassland and mesquite increase with increasing rainfall (NRCS, 1997). Thus, deviations in simulated annual surface runoff between the two scenarios during the wet period will be higher than those in dry episode, leading to higher deviation in annual streamflow during the wet period.

Impacts of mesquite encroachments on hydrological processes were related to meteorological forcing and some geographical properties, including area, elevation and slope. As shown in Table 3, positive correlations between ET and elevation or precipitation were observed, suggesting spatial distribution of elevation or precipitation is the secondary controlling factor of ET besides LULC change. The positive correlation could be due to more water available for evapotranspiration. In addition, negative correlations between other hydrological processes and elevation or precipitation were examined. The negative correlation could also be related to the water availability, i.e. when more rainfall is applied in the upper San Pedro watershed, more significant
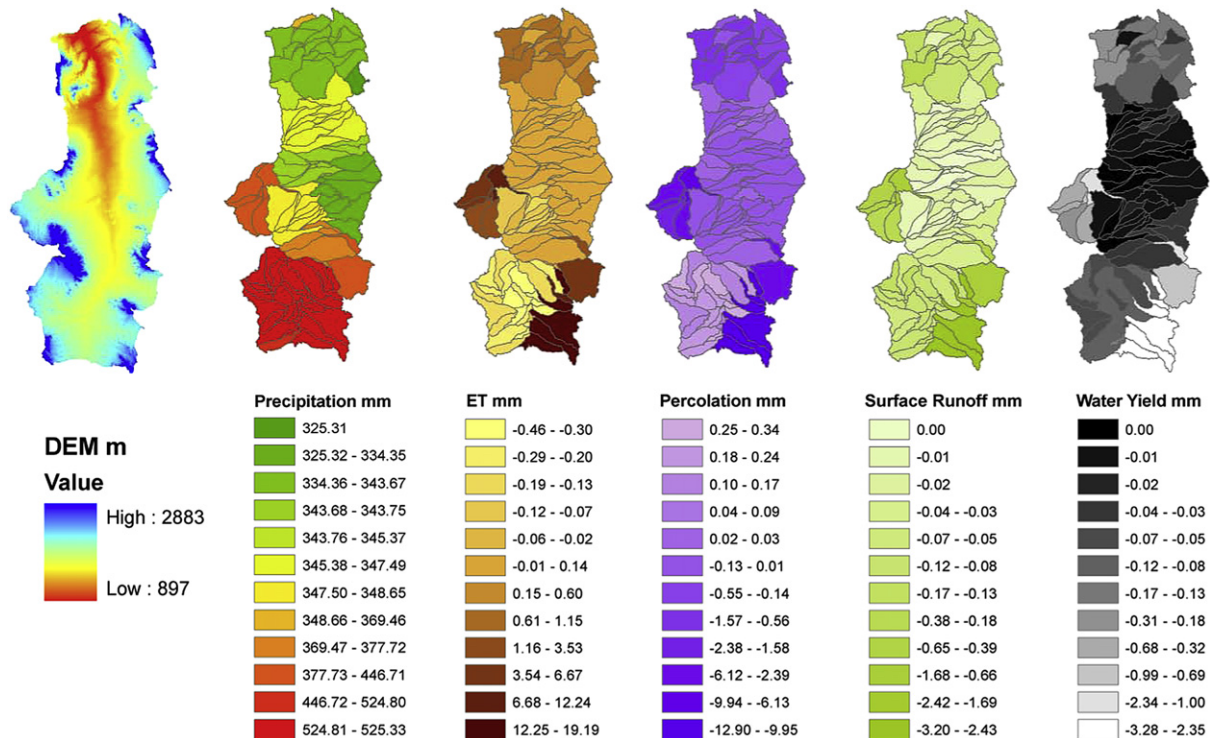

Fig. 5. Spatial distribution of DEM, precipitation, and deviation of four hydrological processes between land use/ land cover Scenario 0 (0% of grassland was replaced by mesquite) and Scenario 10 (100% of grassland was replaced by mesquite).
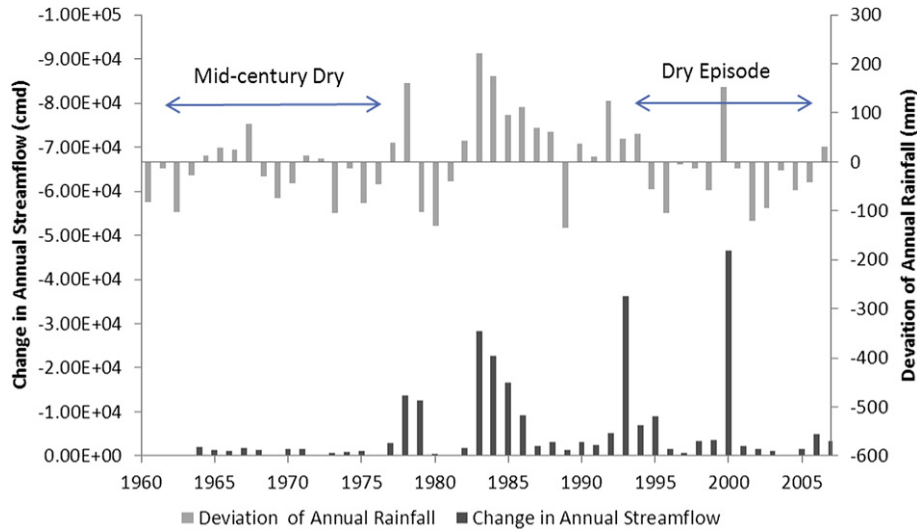
Fig. 6. Relative decrease of simulated annual streamflow in cubic meter per year (between Scenario 0 and Scenario 10) and deviation of annual rainfall from 1960 to 2007. The dry episodes in the upper San Pedro watershed are contemporaneous with observed droughts of Arizona identified using average of monthly records from 25 U.S. historical climate network stations in Arizona (ADRW, 2010).

changes (decreases) in surface runoff, percolation, and water yield should be simulated.

The relationship among three major hydrological processes (runoff, ET, and percolation) and percentage of grassland removed in the upper San Pedro River basin are plotted in Figs. 7 and 8. It shows that complete replacement of grassland with mesquite increases the simulated annual averaged basin ET from 384.3 to 386.1 mm and decreases the annual averaged basin runoff amount from 2.66 to 2.35 mm. Full encroachment of mesquite into grassland reduces annual averaged basin percolation from 13.35 to 12.05 mm. The change of basin annual averaged values of ET, percolation, and surface runoff are not substantial a (few millimeters). However, considering the effects of spatial heterogeneity and weather condition (wet versus dry), impacts of mesquite encroachments on hydrology could still be significant for subwatersheds with more mesquite encroachments in wet periods.

The increased ET with mesquite encroachment can be attributed to the higher transpiration demand of mesquite relative to grassland. The quantification of ET for different riparian species in the upper San Pedro River basin suggested that mesquite woodlands have much higher annual ET rates than grasslands (Scott et al., 2006). Unlike the shallow rooted grassland, mesquite has a shallow lateral root system and a deep vertical root system, which enables it to use water in shallow and deep soils, as well as in the groundwater system (Heitschmidt et al., 1988; Scott et al., 2006). This ability enhances the capacity of mesquite to compete for water

with grassland and other shallow-rooted plants in subbasins with a shallow water table, such as riparian settings. In uplands, studies also show that water yield of rangeland could be significantly increased through controlling brush, such as honey mesquite (Hibbert, 1983). It was indicated that ET of the mesquite treated watershed was significantly lower than ET of the nearby nontreated one (10%–17%) in the North Concho River watershed near San Angelo, Texas, especially during growing seasons (Saleh et al., 2009). The increase of ET changes the water balance, leading to less water to percolate through the bottom of soil and consequently decreasing groundwater supply.

The higher ET due to mesquite encroachment can also impact the volume of surface runoff. Given that more precipitation evapotranspirated, less moisture would remain in the soil after rainfall events, resulting in higher demand of water to saturate the top soil layers before generating any runoff in the next rainfall event. In the SWAT model, the value of Curve Number is justified based on antecedent soil moisture condition before surface runoff is calculated. Consequently, less runoff could be expected with higher ET due to mesquite encroachment into grassland.

A noticeable non-linear response of hydrology to grassland removal can be observed, i.e. hydrological processes changed

Table 3
Pair-wise Pearson correlation for four physical parameters (area, elevation, slope, and precipitation) and changes of four hydrological processes (ET, percolation, surface runoff, and water yield) between land use/ land cover Scenario 0 (0% of grassland was replaced by mesquite) and Scenario 10 (100% of grassland was replaced by mesquite).

	Area	Elevation	Slope	PRECIP	ET	PERC	SURQ	WYLD
Area	1.00							
Elevation	**0.23**	1.00						
Slope	**0.29**	0.14	1.00					
PRECIP	0.00	**0.60**	−0.21	1.00				
ET	0.16	**0.31**	0.07	**0.37**	1.00			
PERC	−0.15	**−0.30**	−0.08	**−0.36**	**−1.00**	1.00		
SURQ	−0.17	**−0.31**	−0.02	**−0.43**	**−0.98**	**0.98**	1.00	
WYLD	−0.16	**−0.32**	−0.06	**−0.42**	**−0.98**	**0.99**	**0.99**	1.00

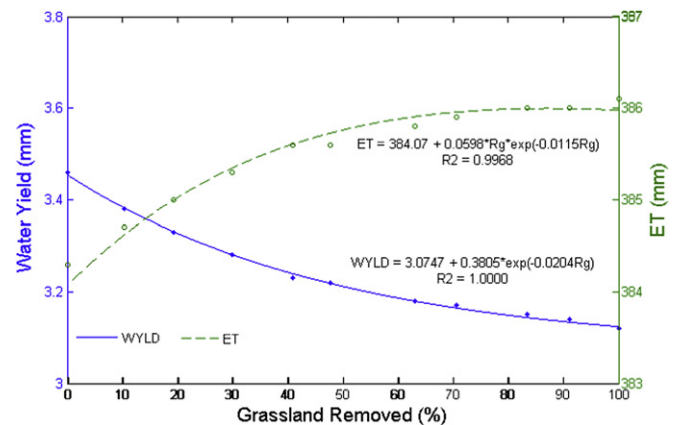$n = 116$, bold numbers are for $p < 0.05$.

Fig. 7. Water yield and ET plotted against percentage of grassland removed (Rg) for the period from 1960 to 2008 based on progressive encroachment of mesquite scenarios.
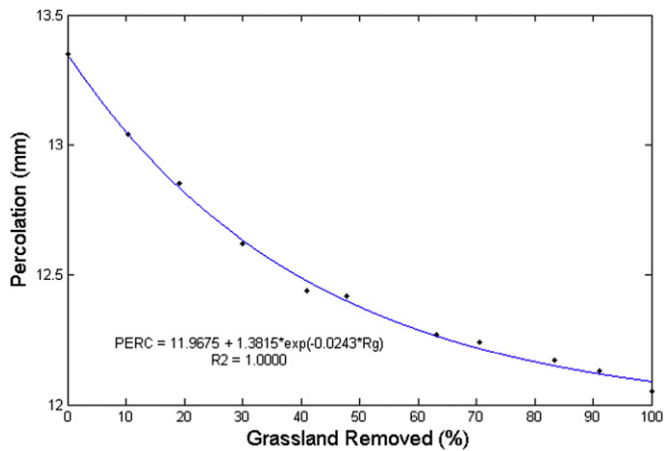
Fig. 8. Precolation (PERC) plotted against percentage of grassland removed (Rg) for the period from 1960 to 2008 based on progressive encroachment of mesquite scenarios.

markedly until a certain amount of grassland was removed (Figs. 7 and 8). For example, the decrease of water yield before a certain percentage (approximately 40%, estimated by the switch of the slope from −0.005 to −0.001) of grassland was removed is much faster than after. Thus, the certain percentage of grassland removal is a threshold of water yield responses to mesquite encroachment. The sensitivity of hydrological responses to landscape change rapidly decreases when the percentage grassland removal exceeds a certain amount (a threshold). It indicates that the strongest response of hydrology to grassland removal occurred in the earliest stage of mesquite encroachment.

The non-linear relationship between hydrology and landscape change was also observed by other researchers (Ghaffari et al., 2010; Li et al., 2007; Zehe and Sivapalan, 2009). The slower hydrological responses in the second stage of mesquite encroachment (after a certain amount of grassland removal) are probably because the evapotranspiration has reached its maximum capacity. The ratio of ET over total precipitation (rainfall and snowmelt) is 95.4% when a certain amount of grassland was replaced by mesquite. Although the evapotranspiration capability increases with mesquite encroachment, presumably because of its higher leaf area index, the actual amount of transpired water does not greatly increase because of the limited available water for transpiration.

5. Summary and conclusions

Progressive encroachments of mesquite into grassland from 0−100% were simulated using the SWAT model for the upper San Pedro watershed to investigate hydrological consequences of mesquite encroachment in a semiarid system. The simulation results show that the annual average basin ET increases with the removal of grassland, while surface runoff and percolation decreases with mesquite encroachment. Impacts of mesquite encroachment on hydrology are more significant for subwatersheds with more grassland replaced by mesquite during wet periods. Notably, simulation results also indicate a non-linear relationship between hydrological response and mesquite encroachment, i.e. the impact on the simulated hydrological processes is significant when grassland removal is below a threshold.

An increase of ET will lead to the decrease of the local or regional water supply because the total amount of water supply (the sum of surface water and groundwater flow) is equal to precipitation (including snow melt) minus ET. In this study, although only a 1.8 mm increase of annual average basin ET was simulated when grassland

was fully replaced by mesquite in the upper San Pedro Watershed, the simulated total runoff (water yield) and percolation decreased by 9.8% and 9.7%, respectively. In addition, a substantial increase in ET (up to 19.19 mm) and decrease of percolation and surface runoff (to −12.90 and −3.20 mm, respectively) were observed in the southeast, middle-west, and northern subwatersheds. The most significant decrease of surface runoff (around 35.8%) was simulated during wet periods. The increase of ET in the arid or semiarid regions is likely to develop a positive feedback that will reinforce the encroachment of mesquite into grassland. When the replacement of grassland by mesquite begins, less soil moisture is available for the ecosystem because the transpiration by mesquite is much higher than grassland. The non-linear relationship between mesquite encroachment and hydrological response indicates that the strongest increase of ET occurred in the early stages of encroachment.

The work associated with this study was intended to provide information to land managers concerned about future ecosystem condition within the context of a large watershed. It was especially focused at issues related to hydrological response as a consequence of potential vegetation change scenarios. Clearly, retrospective analysis using remote sensing has documented that woody plants, such as mesquite, are replacing native desert grasses as the dominant life form. Historically, land managers have engaged in woody plant control activities, e.g. controlled fires, herbicide treatments, and mechanical manipulation, however the most impact can be realized if such actions are engaged during the earliest stages of encroachment.

References

ADRW, 2010. Arizona Water Atlas, vol. 1. Appendix E: Arizona Climate and Drought.
Arnold, J.G., Allen, P.M., Bernhardt, G., 1993. A comprehensive surface-groundwater flow model. Journal of Hydrology 142, 47−69.
Arnold, J.G., Fohrer, N., 2005. SWAT2000: current capabilities and research opportunities in applied watershed modelling. Hydrological Processes 19, 563−572.
Arnold, J.G., Srinivasan, R., Muttiah, R.S., Williams, J.R., 1998. Large area hydrologic modeling and assessment − Part 1: Model development. The Journal of the American Water Resources Association 34, 73−89.
Bahre, C.J., 1991. A legacy of Change: Historic Impact on Vegetation in the Arizona Borderlands. University of Arizona Press, Tuscon.
Briggs, J.M., Schaafsma, H., Trenkov, D., 2007. Woody vegetation expansion in a desert grassland: prehistoric human impact? Journal of Arid Environments 69, 458−472.
Cataldo, J., Behr, C., Montalto, F., 2005. An Analysis of Transmission Losses in Ephemeral Streams, A Case Study in Walnut Gulch Experimental Watershed. National Center for Housing and Environment, Tombstone, AZ, pp. 1−35.
Ceballos, G., Davidson, A., List, R., Pacheco, J., Manzano-Fischer, P., Santos-Barrera, G., Cruzado, J., 2010. Rapid decline of a grassland system and its ecological and conservation implications. PLOS One 5.
Di Luzio, M., Johnson, G.L., Daly, C., Eischeid, J.K., Arnold, J.G., 2008. Constructing retrospective gridded daily precipitation and temperature datasets for the conterminous United States. Journal of Applied Meteorology and Climatology 47, 475−497.
Gassman, P.W., Reyes, M.R., Green, C.H., Arnold, J.G., 2007. The soil and water assessment tool: historical development, applications, and future research directions. Transactions of the ASABE 50, 1211−1250.
Gesch, D., Oimoen, M., Greenlee, S., Nelson, C., Steuck, M., Tyler, D., 2002. The national elevation dataset. Photogrammetric Engineering and Remote Sensing 68, 829−840.
Ghaffari, G., Keesstra, S., Ghodousi, J., Ahmadi, H., 2010. SWAT-simulated hydrological impact of land-use change in the Zanjanrood Basin, Northwest Iran. Hydrological Processes 24, 892−903.
Ghan, S.J., Shippert, T., Fox, J., 2006. Physically based global downscaling: regional evaluation. Journal of Climate 19, 429−445.

Goslee, S.C., Havstad, K.M., Peters, D.P.C., Rango, A., Schlesinger, W.H., 2003. High-resolution images reveal rate and pattern of shrub encroachment over six decades in New Mexico, USA. Journal of Arid Environments 54, 755–767.

Grover, H.D., Musick, H.B., 1990. Shrubland Encroachment in Southern New-Mexico, USA – an analysis of desertification processes in the American Southwest. Climatic Change 17, 305–330.

Griffiths, P.G., Hereford, R., Webb, R.H., 2006. Sediment yield and runoff frequency of small drainage basins in the Mojave Desert, USA. Geomorphology 74, 232–244.

Gupta, H.V., Sorooshian, S., Yapo, P.O., 1999. Status of automatic calibration for hydrologic models: comparison with multilevel expert calibration. The Journal of Hydrologic Engineering 4, 135–143.

Hargreaves, G.L., Hargreaves, G.H., Riley, J.P., 1985. Agricultural benefits for Senegal River Basin. Journal of Irrigation and Drainage Engineering ASCE 111, 113–124.

Hastings, J.R., Turner, R.M., 1965. The Changing Mile: An Ecological Study of Vegetation Change with Time in the Lower Mile of An Arid and Semi-arid Region. University of Arizona Press, Tucson.

Heitschmidt, R.K., Ansley, R.J., Dowhower, S.L., Jacoby, P.W., Price, D.L., 1988. Some observations from the excavation of honey mesquite root systems. Journal of Range Management 41, 227–231.

Hernandez, M., Kepner, W.G., Semmens, D.J., Ebert, D.W., Goodrich, D.C., Miller, R.C., 2003. Integrating a landscape/hydrologic analysis for watershed assessment, The First Interagency Conference on Research in the Watersheds, pp. 1–6.

Hibbert, A.R., 1983. Water yield improvement potential by vegetation management on western rangelands. Water Resources Bulletin 19, 375–381.

Hooghoudt, S.B., 1940. Bijdrage tot de kennis van enige natuurkundige grootheden van de grond. Versl. Landbouwkd. Onderz. 46, 515–707.

Jackson, R.B., Banner, J.L., Jobbagy, E.G., Pockman, W.T., Wall, D.H., 2002. Ecosystem carbon loss with woody plant invasion of grasslands. Nature 418, 623–626.

Kepner, Edmonds, C.M., Watts, C.J., 2002. Remote Sensing and Geographic Information Systems for Decision Analysis in Public Resource Administration: A Case Study of 25 Years of Landscape Change in a Southwestern Watershed. U.S. Environmental Protection Agency, EPA/600/R-02/039, p. 31.

Kepner, W., Watts, C.J., Edmonds, C.M., Maingi, J.K., Marsh, S.E., Luna, G., 2000. Landscape approach for detecting and evaluating change in a semiarid environment. Environmental Monitoring and Assessment 64, 179–195.

Lane, L.J., 1983. Chapter 19: Transmission Losses. In Soil Conservation Service National Engineering Handbook. U.S. Government Printing Office, Washington, D.C., pp. 19-11–19-21.

Li, K.Y., Coe, M.T., Ramankutty, N., De Jong, R., 2007. Modeling the hydrological impact of land-use change in West Africa. Journal of Hydrology 337, 258–268.

Miller, S.N., Guertin, D.P., Goodrich, D.C., 2007. Hydrologic modeling uncertainty resulting from land cover misclassification. The Journal of the American Water Resources Association 43, 1065–1075.

Monteith, J.L., 1965. Evaporation and environment, 19th Symposia of the Society for Experimental Biology. Cambridge University, London, UK, pp. 205–234.

Moriasi, D.N., Arnold, J.G., Van Liew, M.W., Bingner, R.L., Harmel, R.D., Veith, T.L., 2007. Model evaluation guidelines for systematic quantification of accuracy in watershed simulations. Transactions of the ASABE 50, 885–900.

Nash, J.E., Sutcliffe, J.V., 1970. River flow forecasting through conceptual models. Part I: a discussion of principles. Journal of Hydrology, 282–290.

Neitsch, S.L., Arnold, J.G., Kiniry, J.R., Williams, J.R., 2005a. Soil and Water Assessment Tool. Theoretical Documentation. Version 2005, Temple, TX.

Neitsch, S.L., Arnold, J.G., Kiniry, J.R., Williams, J.R., 2005b. Soil and Water Assessment Tool. Input/Output File Documentation. Version 2005, Temple, TX.

Nie, W., Yuan, Y., Kepner, W., Nash, M.S., Jackson, M., Erickson, C., 2011. Assessing impacts of Landuse and Landcover changes on hydrology for the upper San Pedro watershed. Journal of Hydrology, 1–10.

NRCS, 1997. Part 630-Hydrology, National Engineering Handbook. Washington D.C.

Priestley, C., Taylor, R.J., 1972. Assessment of surface heat-flux and evaporation using large-scale parameters. Monthly Weather Reviews 100, 81–82.

Rallison, R.E., Miller, N., 1981. Past, Present and future SCS Runoff Procedure. Water Resources Publication, Littleton, CO.

Saleh, A., Wu, H., Brown, C.S., Teagarden, F.M., McWilliams, S.M., Hauck, L.M., Millican, J.S., 2009. Effect of brush control on evapotranspiration in the North Concho River watershed using the eddy covariance technique. Journal of Soil and Water Conservation 64, 336–349.

Schlesinger, W.H., Reynolds, J.F., Cunningham, G.L., Huenneke, L.F., Jarrell, W.M., Virginia, R.A., Whitford, W.G., 1990. Biological feedbacks in global desertification. Science 247, 1043–1048.

Scott, R.L., Goodrich, D., Levick, L., 2006. Determining the riparian groundwater use within the San Pedro Riparian National Conservation Area and the Sierra Vista Subwatershed, Arizona. In: Leenhouts, J.M., Scott, R.L. (Eds.), Hydrologic Requirements of and Consumptive Ground-Water Use by Riparian Vegetation along the San Pedro River, Arizona, pp. 107–152. USGS Sci. Invest. Report 2005.

Sharpley, A.N., William, J.R., 1990. EPIC-erosion/productivity impact calculator: I – Model Documentation. USDA Technical Bulletins.

Shiferaw, H., Teketay, D., Nemomissa, S., Assefa, F., 2004. Some biological characteristics that foster the invasion of Prosopis juliflora (Sw.) DC. at Middle Awash Rift Valley Area, north-eastern Ethiopia. Journal of Arid Environments 58, 135–154.

Simanton, J.R., Hawkins, R.H., MohseniSaravi, M., Renard, K.G., 1996. Runoff curve number variation with drainage area, Walnut Gulch, Arizona. Transactions of the ASAE 39 (4), 1391–1394.

Solan, P.G., Morre, I.D., Coltharp, G.B., Eigel, J.D., 1983. Modeling Surface and Subsurface Stormflow on Steeply-sloping Forested Watersheds. Water Resource Inst, Lexington. Report 142. University of Kentucky.

Srinivasan, R., Ramanarayanan, T.S., Arnold, J.G., Bednarz, S.T., 1998. Large area hydrologic modeling and assessment – Part II: Model application. The Journal of the American Water Resources Association 34, 91–101.

Stromberg, J.C., Wilkins, S.D., Tress, J.A., 1993. Vegetation-hydrology models – implications for management of Prosopis-Velutina (Velvet Mesquite) Riparian ecosystems. Ecological Applications 3, 307–314.

USDA, S.C.S., 1972. National Engineering Handbook Section 4 Hydrology.

USEPA, 1993. North American Landscape Characterization (NALC) Research Brief. EPA/600/S-93/0005. Office of Research and Development, Washington, D.C., p. 8.

USGS, 2004. Precipitation History of the Mojave Desert Region, 1893–2001.

van Klinken, R.D., Graham, J., Flack, L.K., 2006. Population ecology of hybrid mesquite (Prosopis species) in Western Australia: how does it differ from native range invasions and what are the implications for impacts and management? Biology Invasions 8, 727–741.

West, C.T., Vásquez-León, M., 2008. Misreading the Arizona landscape: reframing analyses of environmental degradation in Southeastern Arizona. Human Organization 67, 373–383.

Wilson, T.B., Webb, R.H., Thompson, T.L., 2001. Mechanisms of Range Expansion and Removal of Mesquite in Desert Grasslands of the Southwestern United States. RMRS-GTR-81. U.S. Forest Service, Rocky Mountain Research Station, p. 23.

Woodward, D.E., Hawkins, R.H., Jiang, R., Hjelmfelt, A.T., Van Mullem, J.A., Quan, Q.D., 2004. Runoff Curve Number Method: Examination of the Initial Abstraction Ratio. In: Proceedings of the World Water and Environmental Resources Congress and Related Symposis. ASCE Publications, Philadelphia, PA. doi:10.1061/40685(2003)308.

Zehe, E., Sivapalan, M., 2009. Threshold behaviour in hydrological systems as (human) geo-ecosystems: manifestations, controls, implications. Hydrology and Earth System Sciences 13, 1273–1297.

Zeng, N., Neelin, J.D., Lau, K.M., Tucker, C.J., 1999. Enhancement of interdecadal climate variability in the Sahel by vegetation interaction. Science 286, 1537–1540.